

Research Article

Optimization-based UWB positioning with multiple tags for estimating position and rotation simultaneously

Hao Chen^a, Bo Yang^{b,*}, Luyang Li^b, Tao Liu^c, Jiacheng Zhang^b, Ying Zhang^d

^a Changwang School of Honors, Nanjing University of Information Science & Technology, Nanjing 210044, China

^b School of Artificial Intelligence, Nanjing University of Information Science & Technology, Nanjing 210044, China

^c Key Laboratory of Pattern Recognition and Intelligent Information Processing, Institutions of Higher Education of Sichuan Province, Chengdu University, Chengdu 610106, China

^d Department of Medical Physics and Biomedical Engineering, University College London, London WC1E 6BT, UK

ARTICLE INFO

Article history:

Received 29 September 2024

Revised 21 November 2024

Accepted 23 December 2024

Available online 10 January 2025

Keywords:

Robot positioning

UWB sensors

Multiple tags

Position estimation

Rotation estimation

ABSTRACT

Currently, the ultra-wideband (UWB) positioning scheme is widely applied to indoor robot positioning and has achieved high positioning accuracy. However, in some narrow and complex environments, its accuracy is still significantly degraded by the multipath effect or non-line-of-sight situations. In addition, the current single tag-based pure UWB positioning methods only estimate the tag position and ignore the rotation estimation of the robot. Therefore, in this paper, we propose a multiple tags-based UWB positioning method to estimate the position and rotation simultaneously, and further improve the position estimation accuracy. To be specific, we first install four fixed tags on the robot. Then, based on the ranging measurements, anchor positions and geometric relationships between each tag, we design five different geometric constraints and smooth constraints to build a whole optimization function. With this optimization function, both the rotations and positions at each time step can be estimated by the iterative optimization algorithm, and the results of tag positions can be improved. Both simulation and real-world experiments are conducted to evaluate the proposed method. Furthermore, we also explore the effect of relative distances between multiple tags on the rotations in the experiments. The experimental results suggest that the proposed method can effectively improve the position estimation performance, while the large relative distances between multiple tags benefit the rotation estimation.

© 2025 The Author(s). Published by Elsevier B.V. on behalf of Shandong University. This is an open access article under the CC BY-NC-ND license (<http://creativecommons.org/licenses/by-nc-nd/4.0/>).

1. Introduction

Autonomous robots have become a popular research topic over the last few decades. We have seen an increasing demand for robots in various applications, such as autonomous driving [1], inspection [2], search and rescue [3]. One of the fundamental technologies for autonomous tasks is positioning. Among the numerous existing positioning solutions, ultra-wideband (UWB) positioning method has emerged as a promising solution due to its high accuracy and reliability, particularly in indoor environments which lack satellite signals [4].

In terms of the 3D UWB positioning, typically, there will be at least four UWB sensors as anchors installed in the environment, and one UWB sensor as tag installed on the robot [5]. Through the communication between UWB sensors, the distances between each anchor and tag in different time steps can be obtained by the tag, while the positions of the anchors are fixed and pre-calibrated. If the ranging measurements are accurate,

the tag positions can be accurately calculated with the distance information and the anchor positions based on the least squares method [6].

However, in narrow and complex indoor environments with some obstructions, the multipath effects and non-line-of-sight (NLOS) situations produce ranging noise which is hard to estimate and filter, thus significantly degrades ranging accuracy [7]. The tag position is also difficult to accurately calculate due to these large ranging errors. Calculating the accurate tag positions in a complex environment is still a challenging issue for UWB positioning [8–11].

Recently, many efforts have been made to improve the UWB positioning accuracy in complex environments. The Kalman Filter algorithm [8], optimization algorithm [9] and some evolutionary algorithms [10,11] are all developed for accurate positioning with large ranging errors. Among them, the optimization algorithm, which first builds the optimization function based on the geometric relationships between anchors and tag and then estimates the tag positions with iterative methods achieves the state-of-the-art positioning results. In addition, some learning-based methods such as convolutional neural network [12,13] and long short-term

* Corresponding author.

E-mail address: 003402@nuist.edu.cn (B. Yang).

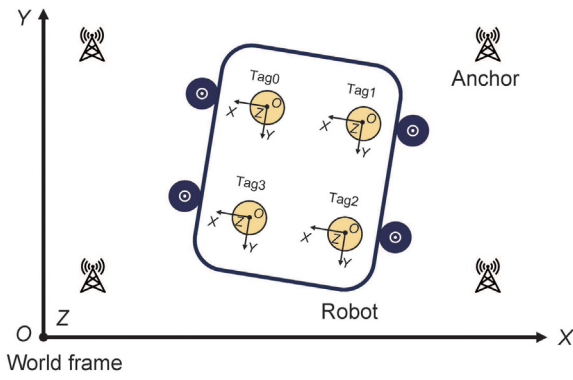


Fig. 1. The diagram of defined frames.

memory [14,15] are also used and obtain the desirable results. However, they require a training process, which needs to pre-collect a few ground-truth trajectories with other more precise and expensive sensors. This requirement limits the transferability of algorithms and environmental adaptability. Therefore, in this paper, we mainly focus on the optimization-based UWB positioning method.

Traditional optimization-based UWB positioning method only places one tag on the robot [9]. At each time step, only one distance can be measured from each anchor. This single-tag strategy is not robust in complex environments and is easily influenced by ranging errors. Another limitation is that the pure single-tag UWB positioning strategy cannot estimate the rotation of the robot, but the rotation information is important for the robot navigation, especially for the aerial robots.

To address these limitations, this paper presents a multi-tag UWB positioning method to improve the positioning performance in complex scenes, and estimate the rotation simultaneously. To be specific, we install four tags on one robot. These four tags form a rectangle, and the positional relationships between each tag are pre-calibrated. Hence, in one time step there will be four distance information from one anchor. These multiple ranging measurements together with the known positional relationships between each tag can improve the robustness and accuracy of the tag estimation. Furthermore, these tags that make up the rectangular shape can help us estimate the rotation, which is always ignored in other UWB positioning methods. In addition, we build both simulation and real-world experiments to evaluate the proposed method. In the experiments, we also vary the relative distance between the tags to see the influence of the position relationships of four tags on rotation estimation.

The main contributions of this work are summarized as follows:

- (1) The multi-tags strategy is proposed for the UWB positioning to improve the accuracy of tag position estimation.
- (2) The rotation estimation method is proposed for the UWB positioning based on the multiple tags. To the best of our knowledge, it is the first method to estimate the UWB tag rotation.
- (3) Both simulation and real-world experiments are designed to illustrate the advantages of the proposed method. The influence of the position relationships of four anchors on position and rotation estimation is also evaluated.

2. Proposed method

The goal of our proposed method is to estimate the 3D pose of the mobile robot with respect to a world frame of reference based on the pure UWB sensors. For the world frame $\{W\}$, we manually set a point as the origin in the environment and establish a

fixed and invariant three-dimensional coordinate system. The pre-calibrated anchor positions and the 3D pose of the robot are all calculated based on this frame. In terms of the robot frame $\{B_0\}$, since we install four tags on the robot, we select the position of tag 0 as the origin of robot frame. The x -axis of robot frame points to the right of the robot, while the y -axis of robot frame points to the front of the robot, and the z -axis is perpendicular to the xy -plane. Except for tag 0, we define three additional frames $\{B_1\}$, $\{B_2\}$, and $\{B_3\}$ for the remaining tags. The origin points of these frames are located at the positions of tag 1, tag 2 and tag 3. Three axes of these frames are parallel to the robot frame $\{B_0\}$. These defined frames are shown in Fig. 1.

2.1. Estimation of position

In this part, we briefly review the optimization-based position estimation method with single UWB tag.

We use the $\mathbf{A}_n \in \mathbb{R}^{3 \times 1}$ to represent the n th anchor position in the world frame, while the $\mathbf{P}_k^W \in \mathbb{R}^{3 \times 1}$ is used to represent the tag positions at time step k in the world frame. In addition, the ranging measurements between the n th anchor and tag at time step k are represented as $d_{n,k}$.

According to the geometric relationship of the \mathbf{A}_n , \mathbf{P}_k^W and $d_{n,k}$, the optimization function of optimization-based UWB positioning method can be built as follows [9].

$$r_{p,k} = d_{n,k} - \|\mathbf{P}_k^W - \mathbf{A}_n\|_2 \quad (1)$$

$$F_p = \min_{\mathbf{P}_k^W} \sum_{n,k} \rho \left(\|r_{p,k}\|_{\Sigma_n^k}^2 \right) \quad (2)$$

where $r_{p,k}$ is the ranging measurement constraint provided by the UWB sensor. Σ_n^k represents the measurement covariance between the n th anchor and the tag at time step k . It can be determined based on the parameters of the UWB sensor. Meanwhile, the Huber kernel function $\rho(\cdot)$ is also introduced to improve the robustness of optimization.

In addition, the UWB positioning is a continuous process, thus, the smooth position constraints between two timesteps can also be introduced. In [9], a weak constraint based on the motion speed of the robot is presented as follows.

$$r_{v,k} = \|\mathbf{P}_k^W - \mathbf{P}_{k-1}^W\|_{\Sigma_{k-1,p}^k}^2 \quad (3)$$

where $\Sigma_{k-1,p}^k$ is defined as the covariance matrix with respect to velocity as follows.

$$\Sigma_{k-1,p}^k = \frac{s}{\Delta t \|V_{max}\|^2} \quad (4)$$

where V_{max} denotes the maximum velocity of the robot. Δt represents the time interval between time step $k-1$ and k . Besides, since the F_v is a weak constraint, the weight of this term can be adjusted by a scaling factor s .

This constraint can improve the positioning accuracy and make the robot's estimated trajectory smoother. Thus, the whole optimization function can be defined as follows.

$$F_{pv} = \min_{\mathbf{P}_k^W} \sum_k \left(\sum_n \rho \left(\|r_{p,k}\|_{\Sigma_n^k}^2 \right) + r_{v,k} \right) \quad (5)$$

Based on the above optimization function, the Gauss–Newton iteration method or the Levenberg–Marquardt algorithm [16] can be used to estimate the tag position at each time step.

2.2. Estimation of rotation

In this part, we will detail the method to estimate the rotation of the robot frame $\{B_0\}$ with respect to the world frame $\{W\}$.

Firstly, we use $\mathbf{P}_{i,k}^W \in \mathbb{R}^{3 \times 1}$ to represent the 3D position of i th tag at time step k in the world frame. Besides, we use the $\mathbf{R}_k^W \in \mathbb{R}^{3 \times 3}$ to represent the rotation matrix from the robot frame to the world frame at time step k . Note that \mathbf{R}_k^W can also represent the rotation matrix from each tag frame to the world frame, since the three axes of all tag frames are parallel to the robot frame. In addition, the $\mathbf{T}_{B_i,k}^W \in \mathbb{R}^{4 \times 4}$ defined as follows are used to represent the transformation matrix from the frame $\{B_i\}$ to the world frame.

$$\mathbf{T}_{B_i,k}^W = \begin{bmatrix} \mathbf{R}_k^W & \mathbf{P}_{i,k}^W \\ \mathbf{0} & 1 \end{bmatrix} \quad (6)$$

Finally, the geometric relationships between tag 0 and the other three tags can be represented as the $\mathbf{T}_{B_i}^{B_0}$ which can be defined as follows.

$$\mathbf{T}_{B_i}^{B_0} = \begin{bmatrix} \mathbf{I} & \mathbf{P}_i^{B_0} \\ \mathbf{0} & 1 \end{bmatrix} \quad (7)$$

where $\mathbf{P}_i^{B_0}$ denotes the position of i th tag in the robot frame. Since all the tags are fixed on the robot, the $\mathbf{P}_i^{B_0}$ can be pre-calibrated, while the rotation between robot frame and each tag frame is the identity matrix \mathbf{I} . Therefore, the $\mathbf{T}_{B_i}^{B_0}$ is a known value that can be used to provide the rotation constraint for rotation estimation.

The $\mathbf{T}_{B_i}^{B_0}$ can be expressed as

$$\mathbf{T}_{B_i}^{B_0} = (\mathbf{T}_{B_0,k}^W)^{-1} \mathbf{T}_{B_i,k}^W \quad (8)$$

Then, Eq. (8) can be expanded as follows.

$$\begin{bmatrix} \mathbf{I} & \mathbf{P}_i^{B_0} \\ \mathbf{0} & 1 \end{bmatrix} = \begin{bmatrix} (\mathbf{R}_k^W)^{-1} & -(\mathbf{R}_k^W)^{-1} \mathbf{P}_{0,k}^W \\ \mathbf{0} & 1 \end{bmatrix} \begin{bmatrix} \mathbf{R}_k^W & \mathbf{P}_{i,k}^W \\ \mathbf{0} & 1 \end{bmatrix} \quad (9)$$

Thus, we obtain

$$\mathbf{P}_i^{B_0} = (\mathbf{R}_k^W)^{-1} \mathbf{P}_{i,k}^W - (\mathbf{R}_k^W)^{-1} \mathbf{P}_{0,k}^W \quad (10)$$

When we multiply \mathbf{R}_k^W on both sides of Eq. (10), we obtain

$$\mathbf{R}_k^W \mathbf{P}_i^{B_0} + \mathbf{P}_{0,k}^W - \mathbf{P}_{i,k}^W = \mathbf{0} \quad (11)$$

where \mathbf{R}_k^W is the rotation that needs to be estimated, $\mathbf{P}_i^{B_0}$ is the known value. $\mathbf{P}_{0,k}^W$ and $\mathbf{P}_{i,k}^W$ can be estimated first by the optimization-based position estimation method introduced in Section 2.1.

Thus, the optimization function for rotation estimation can be built as follows.

$$\mathbf{r}_{R,k} = \mathbf{R}_k^W \mathbf{P}_i^{B_0} + \mathbf{P}_{0,k}^W - \mathbf{P}_{i,k}^W \quad (12)$$

$$F_R = \min_{\mathbf{R}_k^W} \sum_{i,k} \rho \left(\|\mathbf{r}_{R,k}\|_{\sum_i^k}^2 \right) \quad (13)$$

where $\mathbf{r}_{R,k}$ is the rotation constraint. \sum_i^k denotes the measurement covariance, which can be determined empirically based on the accuracy of position estimation.

Finally, the Gauss-Newton iteration method or the Levenberg-Marquardt algorithm can also be used to estimate the rotation at each time step. Note that during the iterative estimation process, the rotation matrix will be mapped to the Lie algebra, and the perturbation model will be used to simplify the optimization process. After the estimation, it will be returned to the rotation matrix.

2.3. Simultaneous estimation of position and rotation with multiple tags

Based on the previous two subsections, we can build a whole optimization function to estimate the position and rotation simultaneously.

The basic function can be constructed as follows.

$$r_{p,i,k} = d_{n,i,k} - \|\mathbf{P}_{i,k}^W - \mathbf{A}_n\|_2 \quad (14)$$

$$r_{v,i,k} = \|\mathbf{P}_{i,k}^W - \mathbf{P}_{i,k-1}^W\|_{\sum_{k-1}^k}^2 \quad (15)$$

$$F_{pvR} = \min_{\mathbf{P}_k^W, \mathbf{R}_k^W} \sum_{i,k} \left(\sum_n \rho \left(\|r_{p,k}\|_{\sum_n^k}^2 \right) + r_{v,i,k} + \rho \left(\|\mathbf{r}_{R,k}\|_{\sum_i^k}^2 \right) \right) \quad (16)$$

where Eqs. (14) and (15) are respectively extended from Eqs. (1) and (3), which are considered the multiple tags.

Furthermore, since we know the geometric relationships between each tag, we can design a multi-tags constraint between the positions of every tag at the same timestep to improve the estimation performance as follows.

$$r_{m,k} = \|\mathbf{P}_{i,c,k}^W - \mathbf{P}_{i+k,c,k}^W\|_2 - d_{i \rightarrow i+c,k} \quad (17)$$

where $d_{i \rightarrow i+c,k}$ is the distance between the i th tag and the $(i+c)$ th tag at the time step t . Besides, since we use four tags in this paper, $i \in [0, 3]$, and $c \in (i, 3]$.

Finally, we can also consider the smooth rotation constraint at different time steps. It can be built as follows.

$$r_{a,k} = \left\| \text{Euler} \left((\mathbf{R}_{k-1}^W)^{-1} \mathbf{R}_k^W \right) \right\|_{\sum_{k-1,a}^k}^2 \quad (18)$$

where $\text{Euler}(\cdot)$ denotes the transformation from the rotation matrix to Euler angle. $\sum_{k-1,a}^k$ is also defined as the covariance matrix with respect to angle velocity as follows.

$$\sum_{k-1,a}^k = \frac{s'}{\Delta t \|\theta_{max}\|^2} \quad (19)$$

where θ_{max} denotes the maximum angle velocity of the robot, while s' is the scaling factor to adjust the weight of this constraint.

Therefore, the final optimization function can be defined as follows.

$$F = \min_{\mathbf{P}_k^W, \mathbf{R}_k^W} \sum_k \left(\sum_i \left(\sum_n \rho \left(\|r_{p,k}\|_{\sum_n^k}^2 \right) + r_{v,i,k} + \rho \left(\|\mathbf{r}_{R,k}\|_{\sum_i^k}^2 \right) + r_{m,k} \right) + r_{a,k} \right) \quad (20)$$

Finally, the rotation and position of the robot can be estimated with the iterative optimization algorithm.

The whole proposed optimization scheme for UWB positioning with multiple tags can be shown in Fig. 2. In this paper, we consider 10 time steps for every optimization ($k = 10$), thus a sliding window is utilized to take the ranging measurements (adding new data and deleting the oldest). In addition, after the estimation, only the last position and rotation results in the sliding window are recorded to represent the current results.

For this scheme, the multiple tags can provide more information, and we fully consider every geometric constraint contained in this system. Hence, the rotation and position can be estimated simultaneously, while the position estimation results are also improved compared to the single-based UWB positioning method. We evaluate the proposed method in Sections 3 and 4.

3. Simulation experiment

3.1. Experiment setting

In the simulation experiment, four tags on the robot are at the same height and form a square shape. We first determine the relative distances between each tag. In this experiment, we separately set two different values: $d_1 = 0.3 \text{ m}$ and $d_2 = 1 \text{ m}$ to

Table 1
Positions of anchors in simulation experiment (m).

Anchor number	Coordinate values
Anchor 0	(0, 0, 0)
Anchor 1	(20, 20, 3)
Anchor 2	(-10, 20, -2)
Anchor 3	(-15, -15, 1)
Anchor 4	(18, -10, -1)
Anchor 5	(10, 10, 1.5)

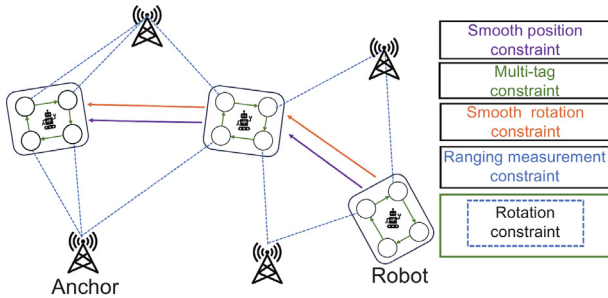


Fig. 2. The whole proposed optimization scheme for UWB positioning with multiple tags. The ranging measurement constraint, rotation constraint, multi-tags constraint and two smooth constraints are all considered in this scheme.

evaluate the influence of different relative distances on the rotation estimation. Secondly, we randomly generate six sequences including continuous position and rotation information for tag 0 on the robot, and calculate the trajectories of the other three tags. Next, based on these trajectories, we generate six 3D positions of anchors to ensure that all the robot trajectories can be surrounded by these anchors. The specific positions of these six anchors are shown in Table 1. Then, the ground-truth distances between all the tags at each time step and the anchors can be calculated. Finally, we add two different Gaussian random noises $\sigma_1 \sim N(0.1, 0.1)$ and $\sigma_2 \sim N(0.1, 0.2)$ to the ground-truth distances of four tags to simulate the UWB ranging measurements, respectively.

In terms of the competing method, the optimization-based UWB positioning method with the single tag [9] is used to compare with the proposed multiple tags scheme for position estimation. This method achieves the state-of-the-art position estimation results among the traditional methods. In addition, for the rotation estimation, since there are no pure UWB positioning scheme can estimate the rotation, we only present the results of rotation estimation in this paper, and explore the influence of the relative distance of tags on rotation estimation.

Besides, the root mean square error (RMSE) is selected as the evaluation metric to assess the position and rotation estimation results in this paper. Note that we only calculate the RMSE for tag 0 of our proposed method as the robot positions to compare with the position estimation results of single tag-based scheme.

Finally, the whole method is implemented in C++, while the optimization process is implemented based on Ceres. The positioning frequency is 10 Hz, the V_{max} is set as 1 m/s, while the θ_{max} is set as $5^\circ/s$.

3.2. Results

The results of simulation experiments with different relative distances between each tag and Gaussian random noise are shown in Table 2, Table 3, Tables 4 and 5, respectively. In addition, we also give the position estimation error curves of S-2 sequence with d_2 and σ_1 parameters of both single tag-based and multiple tags-based method in Fig. 3.

Table 2
RMSE of our proposed method and competing methods with d_1 and σ_1 .

Sequence	Single tag	Multiple tags	
	Position (m)	Position (m)	Rotation ($^\circ$)
S-1	0.130	0.106	25.168
S-2	0.127	0.104	24.960
S-3	0.128	0.103	24.900
S-4	0.129	0.105	24.929
S-5	0.128	0.106	25.260
S-6	0.129	0.103	24.534

Table 3
RMSE of our proposed method and competing methods with d_1 and σ_2 .

Sequence	Single tag	Multiple tags	
	Position (m)	Position (m)	Rotation ($^\circ$)
S-1	0.256	0.205	57.323
S-2	0.259	0.205	57.837
S-3	0.257	0.201	58.930
S-4	0.254	0.207	57.239
S-5	0.251	0.205	57.480
S-6	0.255	0.197	58.991

Table 4
RMSE of our proposed method and competing methods with d_2 and σ_1 .

Sequence	Single tag	Multiple tags	
	Position (m)	Position (m)	Rotation ($^\circ$)
S-1	0.130	0.102	6.805
S-2	0.127	0.101	6.832
S-3	0.128	0.103	6.885
S-4	0.129	0.104	6.914
S-5	0.128	0.103	6.926
S-6	0.129	0.103	6.926

Table 5
RMSE of our proposed method and competing methods with d_3 and σ_1 .

Sequence	Single tag	Multiple tags	
	Position (m)	Position (m)	Rotation ($^\circ$)
S-1	0.256	0.207	13.930
S-2	0.259	0.208	14.193
S-3	0.257	0.206	14.104
S-4	0.254	0.206	14.149
S-5	0.251	0.200	13.868
S-6	0.255	0.203	14.030

In terms of the position estimation, it is clear that the proposed multi-tags scheme is better than the traditional single-tag scheme. We attribute this improvement to the more information provided by multiple tags and our designed multi-tags constraint. These two aspects introduce more useful geometric information to the UWB position estimation, thus improving the accuracy. In addition, the different relative distances between each tag do not influence the position estimation accuracy, since the position estimation is independent of these values.

In terms of the rotation estimation, on one hand, when the relative distances between each tag are the same, the accuracy of rotation estimation is related to the accuracy of position estimation. According to Eq. (11), since the rotation estimation is based on position estimation, higher position estimation accuracy leads to better rotation estimation results. On the other hand, when the added Gaussian random noise is the same, our method obtains a better accuracy of rotation estimation when the relative distance of tags is larger. The reason is that larger relative distances between the tags result in greater relative movement when the robot rotates, and this larger relative movement reduces the impact of position errors on rotation estimation, thus improving rotation accuracy.

Table 6
Position of the tags in the robot frame (m).

Tag	Apartment environment	Laboratory environment
$P_1^{B_0}$	(0, -0.215, 0)	(0, -0.923, 0)
$P_2^{B_0}$	(-0.232, -0.236, 0)	(-0.745, -0.900, 0)
$P_3^{B_0}$	(-0.241, 0.010, 0)	(-0.750, -0.010, 0)

Table 7
Positions of anchors in real-world experiment (m).

Anchor number	Apartment environment	Laboratory environment
Anchor 0	(0, 0, 1.05)	(0, 0, 2.11)
Anchor 1	(5.62, -0.25, 1.16)	(0, 4.80, 0.97)
Anchor 2	(0, 1.99, 2.14)	(6.40, 4.80, 2.28)
Anchor 3	(6.41, 1.30, 2.05)	(6.40, 0, 0.83)
Anchor 4	(3.21, -0.80, 1.76)	(6.40, 2.40, 1.24)
Anchor 5	(2.40, 2.01, 1.36)	(0, 2.40, 1.36)

Table 8
RMSE of our proposed method and competing methods in the apartment environment.

Sequence	Single tag	Multiple tags	
	Position (m)	Position (m)	Rotation ($^\circ$)
RA-1	0.249	0.165	30.590
RA-2	0.269	0.176	40.281
RA-3	0.290	0.127	32.036
RA-4	0.243	0.165	37.808
RA-5	0.285	0.179	41.374
RA-6	0.339	0.199	51.119
RA-7	0.313	0.189	44.658
RA-8	0.353	0.207	50.061
RA-9	0.385	0.248	44.236

4. Real-world experiment

4.1. Experiment setting

We conduct the real-world experiments in two different environments: a living room of an apartment and a laboratory. Ten LinkTrack-P UWB sensors are used in both environments. Among them, six are installed in the environments as the anchors, while the other four are installed on the robot. The value of $P_i^{B_0}$ in these two environments are shown in Table 6, while the positions of six anchors in these two environments are shown in Table 7. It can be seen that the relative distances between tags in the laboratory environment are larger than those in the apartment environment.

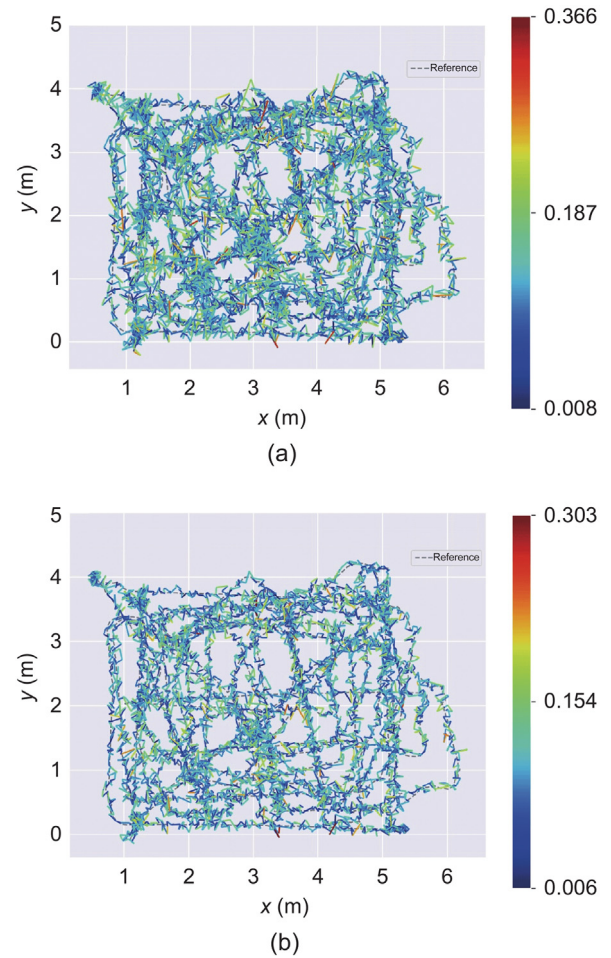
In addition, an RS-Helios-5515 32-line LiDAR is installed on the robot to provide the 3D ground-truth pose by the LOAM method [17] with centimeter-level accuracy. The transformation matrix between the 3D LiDAR and world frame as well as the robot frame are pre-calibrated.

In the experiments, we control the robot to move randomly in the environments, and record both the ranging measurements, estimated positions and rotations and the ground-truth poses.

Finally, the competing method, evaluation metric and implementation are the same as the simulation experiments.

4.2. Results

The results of real-world experiments in two different environments are shown in Tables 8 and 9. In addition, the position estimation error curves of the RA-4 sequence in apartment scene and the RL-5 sequence in laboratory scene of both single tag-based and multiple tags-based method are given in Figs. 4 and 5. The Cumulative Distribution Function (CDF) curves of positioning errors of whole sequences in both two environments are also provided in Fig. 6.

**Fig. 3.** The position estimation error curves of (a) single tag-based method and (b) our proposed method of S-2 sequence with d_2 and σ_1 parameters.**Table 9**
RMSE of our proposed method and competing methods in the laboratory environment.

Sequence	Single tag	Multiple tags	
	Position (m)	Position (m)	Rotation ($^\circ$)
RL-1	0.457	0.224	14.428
RL-2	0.374	0.260	13.363
RL-3	0.371	0.214	12.934
RL-4	0.387	0.221	12.745
RL-5	0.371	0.257	14.605
RL-6	0.302	0.196	12.425

The results of the real-world experiments are consistent with the simulation experiment. In terms of the position estimation, our proposed multiple tags-based method can achieve better estimation performance than the single tag-based method in both two environments, since more tags can provide more information, which benefits the position estimation. In addition, the designed multi-tags constraint is another factor that improves positioning accuracy. The pre-calibrated geometric relationships with different tags are fully introduced through this constraint, leading to an improvement in positioning accuracy.

In terms of the rotation estimation, it also achieves the same results as the simulation experiment. The larger relative distance between each tag, the better accuracy of rotation estimation.

Through the simulation and real-world experiments, the effectiveness of the proposed method is evaluated.

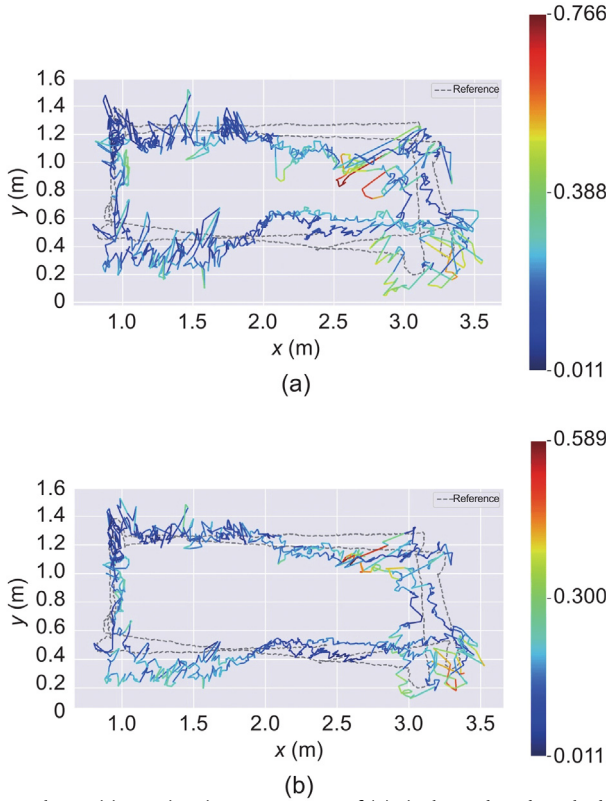


Fig. 4. The position estimation error curves of (a) single tag-based method and (b) our proposed method of RA-4 sequence in the apartment environment.

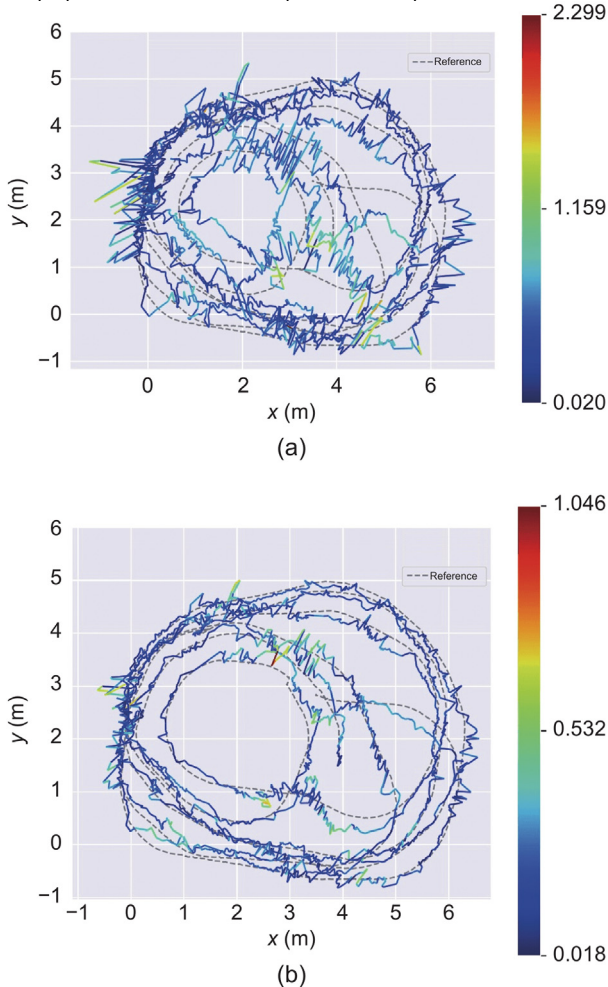
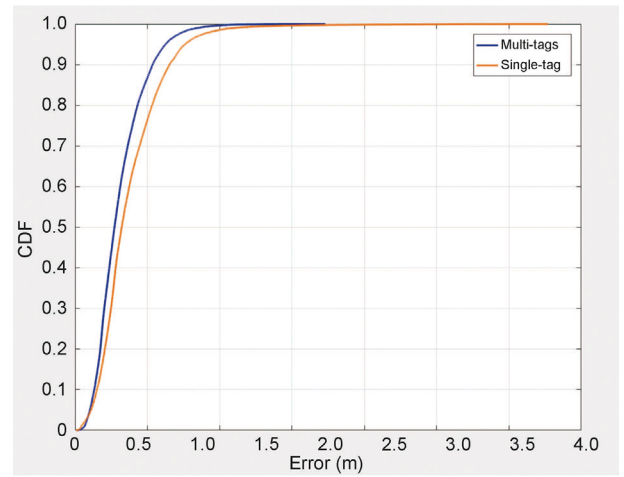
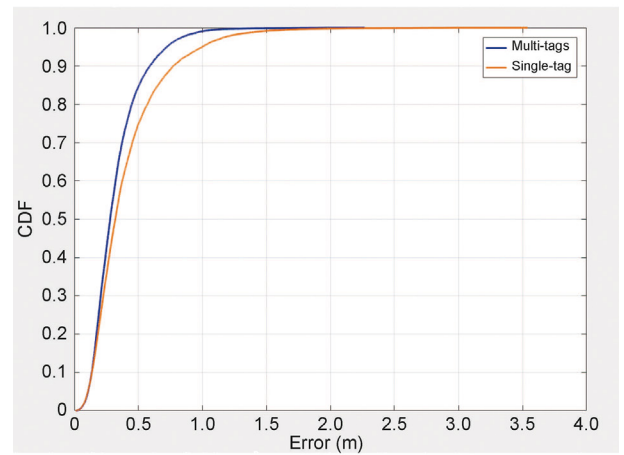


Fig. 5. The position estimation error curves of (a) single tag-based method and (b) our proposed method of RL-3 sequence in the laboratory environment.



(a)



(b)

Fig. 6. The CDF curves of positioning errors of whole sequences in (a) apartment scene (b) laboratory scene.

5. Conclusion and future work

In this paper, we propose an optimization-based UWB positioning with multiple tags for estimating position and rotation simultaneously. For this method, based on the ranging measurements and known information, we mainly design the ranging measurement constraint, rotation constraint, multi-tags constraint and two smooth constraints to build a whole optimization function. The effectiveness of this method is verified through the constructed simulation and real-world experiments. In addition, the influence of the relative distances between the tags on rotation estimation are also explored. The experiments demonstrate that based on the designed optimization function, the accuracy and robustness of UWB position estimation are improved, while better rotation results can be obtained with larger relative distances of tags.

However, although the multiple tags can help the pure UWB positioning method to estimate the rotation of tag. The accuracy of the rotation estimation is limited by the relative distance of tags. In practice, the large relative distance between tags cannot always be guaranteed. Thus, in future work, we will explore fusing the multiple tags UWB information with the data from inertial sensors to further improve the accuracy of position and rotation estimation.

CRedit authorship contribution statement

Hao Chen: Writing – original draft, Software, Methodology, Investigation, Formal analysis. **Bo Yang:** Writing – review & editing, Supervision, Methodology, Funding acquisition, Conceptualization. **Luyang Li:** Software, Investigation. **Tao Liu:** Supervision, Resources. **Jiacheng Zhang:** Supervision, Resources. **Ying Zhang:** Supervision.

Declaration of competing interest

The authors declare that they have no known competing financial interests or personal relationships that could have appeared to influence the work reported in this paper.

Acknowledgments

This work was supported in part by the National Natural Science Foundation of China (62303230), in part by the Key Laboratory of Pattern Recognition and Intelligent Information Processing, Institutions of Higher Education of Sichuan Province (MSSB-2024-05).

References

- [1] C. Li, W. Penghao, C. Kashyap, J. Bernhard, G. Andreas, L. Hongyang, et al., End-to-end autonomous driving: Challenges and frontiers, *IEEE Trans. Pattern Anal. Mach. Intell.* (2024) 1–20.
- [2] Srijeet Halder, Kereshmeh Afsari, Robots in inspection and monitoring of buildings and infrastructure: A systematic review, *Appl. Sci.* (4) (2023) 2304.
- [3] S. Solmaz, et al., Robust robotic search and rescue in harsh environments: An example and open challenges, in: *IEEE International Symposium on Robotic and Sensors Environments, ROSE, Chemnitz, Germany, 2024*, pp. 1–8.
- [4] S. Sung, H. Kim, J.I. Jung, Accurate indoor positioning for UWB-based personal devices using deep learning, *IEEE Access* 11 (2023) 20095–20113.
- [5] F. Zhu, K. Yu, Y. Lin, C. Wang, J. Wang, M. Chao, Robust LOS/NLOS identification for UWB signals using improved fuzzy decision tree under volatile indoor conditions, *IEEE Trans. Instrum. Meas.* 72 (2023) 1–11.
- [6] A.-N.K. Jumaah, W. Hashim, A.K. Alami, An effective indoor positioning system by modified linearized least square approach using UWB technology, *Appl. Geomat.* 16 (1) (2024) 17–28.
- [7] D. Feng, et al., An adaptive IMU/UWB fusion method for NLOS indoor positioning and navigation, *IEEE Internet Things J.* 10 (13) (2023) 11414–11428.
- [8] J. Dong, Z. Lian, J. Xu, et al., UWB localization based on improved robust adaptive cubature Kalman filter, *Sensors* 23 (5) (2023) 2669.
- [9] C. Wang, H. Zhang, T.M. Nguyen, et al., Ultra-wideband aided fast localization and mapping system, in: *IEEE International Conference on Intelligent Robots and Systems, IROS, Vancouver, BC, Canada, 2017*, pp. 1602–1609.
- [10] P. Dai, et al., Efficient localization algorithm with UWB ranging error correction model based on genetic algorithm-ant colony optimization-backpropagation neural network, *IEEE Sens. J.* 23 (23) (2023) 29906–29918.
- [11] X. Zheng, An improved genetic algorithm for UWB localization, *J. Comput. Commun.* 10 (10) (2022).
- [12] B. Yang, J. Li, Z. Shao, H. Zhang, Robust UWB indoor localization for NLOS scenes via learning spatial-temporal features, *IEEE Sens. J.* 22 (8) (2022) 7990–8000.
- [13] L. Nosrati, M.S. Fazel, M. Ghavami, Improving indoor localization using mobile UWB sensor and deep neural networks, *IEEE Access* 10 (2022) 20420–20431.
- [14] Y. Tian, Z. Lian, P. Wang, et al., Application of a long short-term memory neural network algorithm fused with Kalman filter in UWB indoor positioning, *Sci. Rep.* 14 (1) (2024) 1–14.
- [15] D.-H. Kim, A. Farhad, J.-Y. Pyun, UWB positioning system based on LSTM classification with mitigated NLOS effects, *IEEE Internet Things J.* 10 (2) (2023) 1822–1835.
- [16] J. Nocedal, J.W. Stephen, *Numerical Optimization*, Springer, New York, NY, 1999.
- [17] J. Zhang, S. Singh, LOAM: lidar odometry and mapping in real-time, in: *Robotics: Science and Systems, 2014*.